

Origin of π -Facial Stereoselectivity in Nucleophilic Additions. Application of the Exterior Frontier Orbital Extension Model to Imines and Iminium Ions

Shuji Tomoda* and Takatoshi Senju

Department of Life Sciences, Graduate School of Arts and Sciences, The University of Tokyo, Komaba, Meguro, Tokyo 153-8902, Japan

Mitsuhiro Kawamura and Takafumi Ikeda

Medical Chemistry Department, Central Research, Pfizer Pharmaceuticals Inc., 5-2 Taketoyo, Aichi 470-23, Japan

Received January 4, 1999

The experimental data of π -facial stereoselection of the imines and the iminium ions of cyclohexanone, tropinone, and adamantan-2-ones have been explained by the exterior frontier orbital extension model (EFOE model) previously proposed. In all cases, facial difference in the π -plane-divided accessible space (PDAS), which represents simple summation of the π -plane-divided exterior three-dimensional space nearest to the reaction center outside the van der Waals surface, significantly depends on the structure of the imino moieties. In particular the formation of iminium salt significantly affects the magnitude of both the EFOE density and the PDAS values.

Introduction

Unraveling the mechanism and stereochemistry of addition reactions to π -bonds has attracted organic chemists' interests for over four decades and has been the subject of diverse investigations.¹ Since Cieplak's proposal of his conceptual model in 1981,² most discussions are focused on the importance of transition state stabilization arising from the *anti*-periplanar hyperconjugative stabilization effect involving the incipient bond.³ Recently we reported a quantitative analysis of the transition states of cyclohexanone reduction with LiAlH₄.^{4,5} It was proposed that the transition state effects, such as torsional strain and the *anti*-periplanar effect, are not essential for facial diastereoselection of nucleophilic additions to various cyclic ketones including adamantan-2-ones. Surprisingly they often operate against observed facial stereoselectivity.⁴

In the present paper, we extend our theoretical approach toward understanding the essential features of π -facial stereoselection based on the exterior frontier orbital extension model (the EFOE model)^{5,6} to the hydride reductions of the imines and iminium ions of cyclohexanone and tropinone and the oxonium ion of 5-fluoroadamantan-2-one.

Computational Methods

The details of the definition of the two parameters of the EFOE model have been described elsewhere.^{5,6} The

EFOE model focuses on the first and third terms of the Salem–Klopman equation (eq 1).⁷

$$\Delta E = - \underbrace{\sum_{ab} (q_a + q_b) \beta_{ab} S_{ab}}_{\text{1st term}} + \underbrace{\sum_{k < l} \frac{Q_k Q_l}{r_{kl}}}_{\text{2nd term}} + \underbrace{\sum_r \sum_s \text{occ. unocc.} - \sum_s \sum_r \text{occ. unocc.} \frac{2(\sum_{ab} c_{ra} c_{sb} \beta_{ab})^2}{E_r - E_s}}_{\text{3rd term}} \quad (1)$$

q_a, q_b = electron density at atom a or b .

β = resonance integral, S = overlap integral

Q_k, Q_l = total electron densities at atom k or l .

r_{kl} = distance between atoms k and l .

E_r = energy level of MO r .

c = MO coefficients

The model is designed for quantitative evaluation of the first (exchange repulsion; steric effects) and the third (orbital interaction; the donor–acceptor stabilizing interaction) terms to identify essential factors of π -facial diastereoselectivity of addition reactions to π -systems in general including ketones, alkenes, and enolates. Two new quantities—the π -plane-divided accessible space (PDAS) as the steric effect term and the exterior frontier

* Corresponding author. Phone: +81 3 5454 6575. Fax: +81 3 5454-6998. E-mail: tomoda@selen.c.u-tokyo.ac.jp.

(1) Gung, B. W. *Tetrahedron* **1996**, *52*, 5263.
 (2) Cieplak, A. S. *J. Am. Chem. Soc.* **1981**, *103*, 4540.
 (3) Cheung, C. K.; Tseng, L. T.; Lin, M.-H.; Srivastava, S.; le Noble, W. J. *J. Am. Chem. Soc.* **1986**, *108*, 1598.
 (4) Tomoda, S.; Senju, T. *Chem. Commun.* **1999**, 423.
 (5) Tomoda, S.; Senju, T. *Tetrahedron* **1999**, *55*, 5303.
 (6) Tomoda, S.; Senju, T. *Tetrahedron* **1997**, *53*, 9057.

(7) (a) Klopman, G. *J. Am. Chem. Soc.* **1968**, *90*, 223. (b) Salem, L. *J. Am. Chem. Soc.* **1968**, *90*, 543. (c) Fleming, I. *Frontier Orbitals and Organic Chemical Reactions*; John Wiley & Sons: London, 1977.

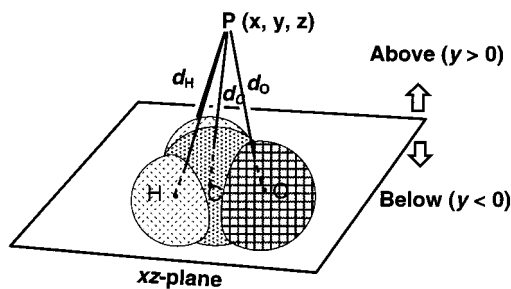


Figure 1. Definition of the π -plane-divided accessible space (PDAS) for formaldehyde molecule.

orbital extension density (EFOE density) as the orbital interaction term—constitute the new model. Both quantities are defined in the exterior area⁸ of a molecule.

The definition of the PDAS is based on the simple assumption that the volume of the outer (exterior) space nearest to a reaction center should contain steric information of the reactant (substrate), since this volume precisely corresponds to the three-dimensional space available for a reagent to access the reaction center of the substrate. The exterior volume is calculated for the two faces of the π -plane separately. Figure 1 illustrates the definition of the π -plane-divided accessible space (PDAS) as a quantitative measure of π -facial steric effects using formaldehyde as an example. The molecular surface is defined as an assembly of spherical atoms having the appropriate van der Waals radii.⁹ Integration of the exterior three-dimensional space for the PDAS of the carbonyl carbon is performed according to the following conditions. If a three-dimensional point $P(x, y, z)$ outside the repulsive surface is the nearest to the surface of the carbonyl carbon (a reaction center on the xz plane) (i.e., if the distance between P and the van der Waals surface of the carbonyl carbon (d_C) is the shortest compared with the distances from P to the other atomic surfaces (two d_H and one d_O)) and if the point is located above the carbonyl plane ($y > 0$), the space at this point is assigned to the above-space of the carbonyl carbon. The integration (summation) of such points is defined as the PDAS of the carbonyl carbon for the above-plane. For the sake of convenience, spatial integration is limited to 5 au (2.65 Å) from the molecular surface, where extension of an electronic wave function is negligible beyond this limit. In general, the carbonyl plane is defined as the plane which includes the two sp^2 atoms of the π -bond and which is parallel with the vector connecting the two atoms at the α -positions.

The third term parameter of the Salem–Klopman equation, namely the π -plane-divided EFOE density (hereafter called simply “EFOE density”) is defined as the integrated (summed) electron density of a frontier orbital (FMO)¹⁰ over specific exterior points over one face of the π -plane of a substrate molecule satisfying the following condition: *the absolute total value of the wave functions belonging to the carbonyl carbon makes a maximum contribution to the total value of FMO wave function at the point.* Such a condition guarantees that the driving force vector on hydride or other reagent is

maximally directed toward the sp^2 reaction center. Thus the integration of the FMO probability density (Ψ_{FMO}^2) over such three-dimensional subspace (Ω) that satisfies the above condition should afford a reasonable quantitative measure of the third term of eq 1. The values of the EFOE density (eq 2) are expressed in % for the sake of numerical convenience by normalizing the wave function (Ψ_{FMO}) to 100.

$$\text{EFOE density (\%)} = 100 \times \int \Psi_{\text{FMO}}^2 d\Omega \quad (2)$$

The computer program was designed so that simultaneous calculation of both the PDAS and the EFOE density could be performed according to the three-dimensional lattice method with a unit lattice volume of 0.008 au³ (1.18×10^{-3} Å³). The quality of each EFOE calculation was checked by the value of the total electron density of the FMO in interest, which converged nearly unity (1.000 ± 0.001). Spatial integration is limited to 5 au (2.65 Å) from molecular surface, where extension of an electronic wave function is negligible beyond this limit. The carbonyl plane is defined as the plane which includes both sp^2 atoms of the π -bond and which is parallel with the vector connecting the two carbon atoms at the α -positions. Bondi’s van der Waals radii⁹ were employed for the definition of molecular surface. The calculation procedure usually begins with structure optimization at the HF/6-31G(d) level using Gaussian 94 followed by a single point calculation with “ginput” and “pop=full” keywords at the same level.¹¹

Results and Discussion

Remarkable predictive power of the EFOE model^{5,6} has been demonstrated in well-known examples of π -facial diastereoselectivity of carbonyl additions for which controversial arguments had been presented.¹

We now report that the EFOE model can be successfully applied to imines and iminium ions as well. A number of reports have appeared to date on the facial stereoselection with respect to the C=N bond in connection with the reductive amination of carbonyl compounds directed toward the total synthesis of natural products.¹² Table 1 shows the EFOE analysis of LUMO’s and observed stereoselectivities for some simple imines and iminium ions of cyclohexanone (**1**) and the relevant data of cyclohexanones for comparison. On going from the

(11) Gaussian 94 (Revision E.2); Gaussian, Inc., Pittsburgh, PA, 1997. Gaussian, Inc., Pittsburgh, PA, 1997; Frisch, M. J.; Trucks, G. W.; Head-Gordon, M.; Gill, P. M. W.; Wong, M. W.; Foresman, J. B.; Johnson, B. G.; Schlegel, H. B.; Robb, M. A.; Replogle, E. S.; Gomperts, R.; Andres, J. L.; Raghavachari, K.; Binkley, J. S.; Gonzalez, C.; Martin, R. L.; Fox, D. J.; Defrees, D. J.; Baker, J.; Stewart, J. J. P.; Pople, J. A., Gaussian, Inc., Pittsburgh, PA, 1992. Gaussian 94 (Revision D.1); Frisch, M. J.; Trucks, G. W.; Schlegel, H. B.; Gill, P. M. W.; Johnson, B. G.; Robb, M. A.; Cheeseman, J. R.; Keith, T.; Peterson, G. A.; Montgomery, J. A.; Raghavachari, K.; Al-Laham, M. A.; Zakrzewski, V. G.; Ortiz, J. V.; Foresman, J. B.; Cioslowski, J.; Stefanov, B. B.; Nanayakkara, A.; Challacombe, M.; Peng, C. Y.; Ayala, P. Y.; Chen, W.; Wong, M. W.; Andres, J. L.; Replogle, E. S.; Gomperts, R.; Martin, R. L.; Fox, D. J.; Binkley, J. S.; Defrees, D. J.; Baker, J.; Stewart, J. P.; Head-Gordon, M.; Gonzalez, C.; Pople, J. A.

(12) (a) Wrobel, J. E.; Ganem, B. *Tetrahedron Lett.* **1981**, 22, 3447. (b) Hutchins, R. O.; Su, W.-Y.; Sivakumar, R.; Cistone, S.; Stercho, Y. P. *J. Org. Chem.* **1983**, 48, 3412. (c) Cabaret, D.; Chauviere, G.; Welvart, Z. *Tetrahedron Lett.* **1966**, 34, 4109. (d) Mattson, R. J.; Pham, K. M.; Leuch, D. J.; Cowen, K. A. *J. Org. Chem.* **1990**, 55, 2552. (e) Abdel-Magid, A. F.; Carson, K. G.; Harris, B. D.; Maryanoff, C. A.; Shah, R. D. *J. Org. Chem.* **1996**, 61, 3849. (f) Cabaret, D.; Chauviere, G.; Welvart, Z. *Tetrahedron Lett.* **1968**, 549. (g) McGill, J. M.; LaBell, E. S.; Williams, M. *Tetrahedron Lett.* **1996**, 37, 3977.

(8) Ohno, K.; Matsumoto, S.; Harada, Y. *J. Chem. Phys.* **1984**, 81, 4447.

(9) Bondi, A. *J. Phys. Chem.* **1964**, 68, 441.

(10) (a) Fukui, K. *Theory of Orientation and Stereoselection*, Springer-Verlag: Heidelberg, 1979. (b) Fukui, K.; Fujimoto, H. *Frontier Orbitals and Reaction Paths*, World Scientific: London, 1997.

Table 1. EFOE Analysis of Cyclohexanone Imines and Iminium Ions (1)^a

	R ₁	R ₂	EFOE Density (%)		PDAS (au ³)		ω^b (au ³)	obsd ^c	
			<i>ax</i>	<i>eq</i>	<i>ax</i>	<i>eq</i>		reagents	<i>ax/eq</i>
		cyclohexanone	1.940	0.249	19.4	47.2	27.8		
		4- <i>t</i> -butylcyclohexanone	1.799	0.249	19.6	46.7	27.1	LiAlH ₄ NaBH ₄ NaBH ₃ CN AlH ₂ (OR') ₂ Na ^d	92:8 ^e 83:17 ^f 84:16 ^f 92:8 ^f
imines (1a)	H		1.367	0.168	14.7	49.8	35.1		
	Me		1.313	0.175	13.3	46.6	33.3		
iminium ions (1a)	H	H	1.170	0.631	14.0	45.5	31.4		
	Me	Me	1.176	0.763	11.0	42.2	31.2	LiAlH ₄ NaBH ₄ NaBH ₃ CN AlH ₂ (OR') ₂ Na ^d	65:35 ^e 84:16 ^f 58:42 ^f 28:72 ^f
	CH ₂ Ph	H	1.270	0.618	13.7	38.1	24.4	NaBH ₃ CN NaBH(OAc) ₃	65:35 ^g 20:80 ^h
	-(CH ₂) ₄ - (pyrrolidinium)		1.286	0.691	12.4	37.5	25.1	NaBH ₄ NaBH ₃ CN AlH ₂ (OR') ₂ Na ^d	86:14 ^f 64:36 ^f 30:70 ^f
	-(CH ₂) ₅ - (piperidinium)		0.926	0.806	9.2	23.1	13.9	LiAlH ₄	64:36 ^e

^a HF/6-31G(d); R = H unless otherwise noted. ^b $\omega = \text{PDAS}(eq) - \text{PDAS}(ax)$. ^c *tert*-Butylcyclohexanone imine (**1b**) (R = *t*-Bu). ^d R' = CH₂CH₂OCH₃. ^e Reference 12c. ^f Reference 12b. ^g Reference 12a. ^h Reference 12g.

Table 2. EFOE Analysis of the Imines and Iminium Ions of Model Tropinone (2m) and Observed Stereoselection of Tropinone (2)^a

2m	R ₁	R ₂	EFOE Density (%)		PDAS (au ³)		ω (au ³) ^b	reagent	obsd for (2) <i>exo:endo</i>
			<i>exo</i>	<i>endo</i>	<i>exo</i>	<i>endo</i>			
tropinone			0.175	1.431	36.1	8.9	27.2	—	—
H		—	0.143	0.672	42.7	5.4	37.3	—	—
Me		—	0.127	1.019	33.5	6.3	27.2	—	—
H		H	0.469	0.852	30.8	8.2	22.6	—	—
Me		H	0.409	1.128	25.8	10.6	15.2	—	—
Me		Me	0.382	1.507	24.5	18.2	6.3	—	—
PhCH ₂ ^{c,d}		—	0.161	0.793	36.2	5.3	30.9	NaBH(OAc) ₃ NaBH ₄ ^e	20:1 ^f 1.5:1 ^f
MeOCOCH ₂ ^c		—	0.873	0.201	31.9	4.8	27.1	NaBH(OR) ₃ ^g	100:0 ^h
Ph ^{c,d}		—	0.425	0.128	18.5	5.3	13.2	NaBH(OAc) ₃	100:0 ^f
piperidine			0.503	1.197	17.5	30.3	-12.8	NaBH ₄ ^e	1:7 ^f
piperazine			0.507	1.116	19.0	27.8	-8.8	NaBH ₄ ^e	1:15 ^h

^a HF/6-31G(d). ^b $\omega = \text{PDAS}(exo) - \text{PDAS}(endo)$. ^c The most stable conformer was selected. ^d LUMO+2. ^e In the presence of Ti(O^{*i*}Pr)₄. ^f Reference 12e. ^g R = 2-ethoxyhexanoyl. ^h Reference 13.

ketone to the NR (R = H, Me) imines, both the PDAS values and the EFOE densities for the *ax*-face decrease (~19 → ~13 au³; ~1.9 → ~1.3%). On going from the imines to the iminium ions ((R₁, R₂) = H or Me), the PDAS values for the axial face (*ax*-face) further decrease (14–13 → 14–9 au³), while the EFOE density values for the equatorial face (*eq*-face) significantly increase (~0.2 → ~0.7%). This is consistent with the observed facial stereoselectivity of the iminium ions listed in Table 1 which shows enhanced equatorial selectivities compared with 4-*tert*-butylcyclohexanone in hydride reduction. It is noted that the stereochemical changes may originate from the skeletal deformation of the iminium ions arising from the hybridization changes of the α -carbons toward sp² owing to the enhanced electron demand from the electron-deficient iminium carbon (hyperconjugation), which is much more electron-deficient than the C=N bond of the imines. For example, comparison between the NH imine (**1**; R₁ = H, R₂ = lone pair) and the NH₂ iminium ion of cyclohexanone (**1**; R₁ = H, R₂ = H) reveals simultaneous bond shortening of C1–C2 (C1–C6) (1.516 → 1.495 Å) and bond elongation of C=N (1.256 → 1.281 Å) due to the hyperconjugation between the $\pi_{\text{C=N}^*}$ and C1–H (C6–H) bonds.

This seems the trend commonly observed for the iminium ions of tropinone (**2**) as described below. Table

2 collects the EFOE data of the imines and the iminium ions of model tropinone (**2m**), in which the *N*-methyl is replaced by hydrogen for computational convenience, along with some experimentally determined stereoselectivity of the reductive amination of tropinone with various amines. In complete agreement with the EFOE data, it has long been known that the hydrogenation of parent tropinone occurs from the less-hindered *exo*-face to give the *endo* alcohol, whereas LiBH₄ reduction takes place preferentially from the *endo*-face: the *endo*-face of model tropinone is much more sterically congested (PDA-S(*exo*) = 8.9 au³) than the *exo*-face (PDAS(*endo*) = 36.1 au³), whereas the EFOE density of model tropinone for the same face (1.431%) is much greater than that of the other face (0.175%).

The EFOE analysis of the imines and the iminium ions of model tropinone (**2m**; R₁, R₂ = H, Me or lone pair) show some interesting features. The imines show analogous trends as model tropinone itself. However, the iminium ions exhibit two notable changes due to considerable skeletal deformation due to enhanced hyperconjugation: the *endo*-face becomes less hindered due to enhanced coplanarity around C-2, C-3, and C-4, while the *endo/exo* ratio of the EFOE density increases. Indeed, as the methyl substitution increases in the iminium ions (C=NH₂ → C=NHMe → C=NMe₂), the PDAS values for the

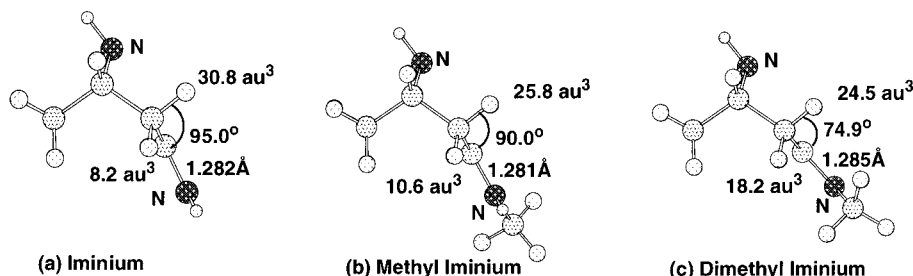


Figure 2. Side views of the optimized structures and the PDAS values of (a) iminium, (b) methyliminium, and (c) dimethyliminium ions of the model tropinone (**2m**) (HF/6-31G(d)).

Table 3. EFOE Analysis of Danishefsky Imine (**3**), Adamantanone Oxonium (**4**), Imine (**5**), and Iminium Ion (**6**)^a

compd no.	EFOE Density (%)		PDAS (au ³)		ω (au ³) ^b	bond length (Å)		obsd A:B
	A	B	A	B		C1-C2	C2-C3	
3	0.222	1.075	4.2	9.3	5.1	—	—	0:100 ^c
adamantan-2-one	1.097	1.098	11.1	11.1	0.0	1.5246	1.5246	50:50
5-F-adamantan-2-one	1.032	1.068	10.3	12.7	2.4	1.5271	1.5271	38:62 ^d
4	0.929	1.236	7.5	11.1	3.6	1.4927	1.4934	17:83 ^e
5	0.793	0.746	9.0	9.8	0.8	1.5183	1.5238	—
6	0.825	0.911	8.4	9.7	1.3	1.5138	1.5139	—

^a HF/6-31G(d). ^b $\omega = \text{PDAS(B)} - \text{PDAS(A)}$. ^c Reduction with NaCNBH₃. Reference 14. ^d Reduction with NaBH₄. Reference 3. ^e Reduction with NaBH₄. Reference 15.

endo-face increase (8.2 \rightarrow 10.6 \rightarrow 18.2 au³). Simultaneously the *endo/exo* ratio of EFOE density increases. It follows that alkyl substitution at the nitrogen of an iminium ion of tropinone should activate the *endo*-face both sterically and electronically. As shown in Figure 2, this changes correspond to the increase in hyperconjugation of methyl as indicated by the increase of the torsion angle between C3=N and C2(C4)-H_{exo} bonds (95.0 \rightarrow 90.0 \rightarrow 74.9°) as methyl substitution increases at the nitrogen.

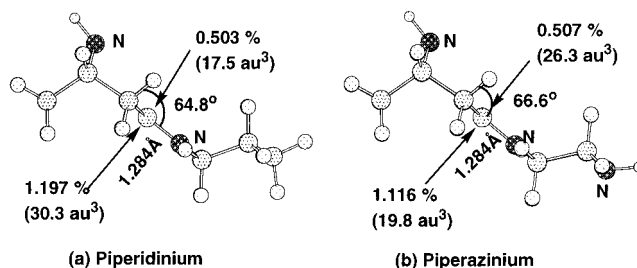
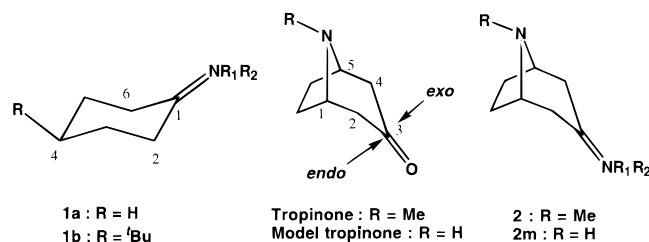


Figure 3. Side views of the optimized structures and the EFOE data of (a) the piperidinium ion and (b) the piperazinium ion of the model tropinone (**2m**). Numbers in % are the EFOE density and PDAS values are indicated in parentheses.



As shown in the last six experimental data of hydride reductions of the imines and the iminium ions listed in Table 2, stereochemical control of the reductive amination of tropinone has been achieved by the use of amines with bulky substituents. The imines of benzylamine,^{12e} glycine,¹³ and aniline^{12e} effectively completely block the *endo*-face (PDAS(*endo*) = \sim 5 au³) and reduce the EFOE density of the *endo*-face to undergo preferentially the *exo*-attack, while secondary amines, such as piperidine^{12e} or piperazine,¹³ make the *endo*-face much less hindered and more reactive as predicted not only by the PDAS values of the piperidinium and piperazinium ions (PDAS (*endo*)

= 30.3 and 27.8 au³, respectively) but also by the EFOE densities of the *endo*-face (1.197 and 1.116%, respectively) to give the *endo* products predominantly.¹³ As shown in Figure 3, the torsion angle between C3=N and C2(C4)-H_{exo} bonds of the structures of these two iminium ions optimized at the HF/6-31G(d) level are only 64.8° and 66.6° for the piperidinium and piperazinium ions, respectively, to make the three-carbon bridge (C1-C2-C3-C4-C5) nearly coplanar with the C=N bond. This strongly indicates that conformational deformation due to hyperconjugation is responsible for the remarkable change of facial stereoselection for these iminium ions.

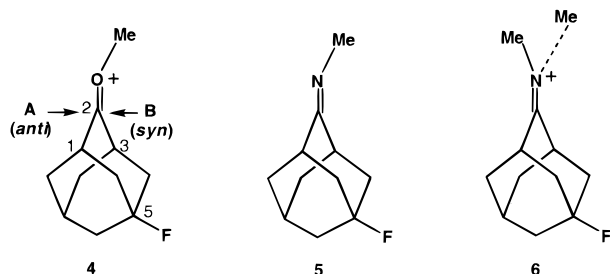
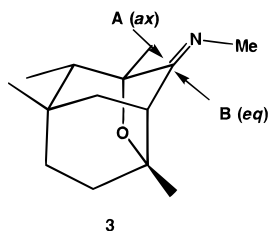
A few interesting examples of facial selection of imines, oxonium ions, and iminium ions have been recently reported.^{14,15} Table 3 collects the results of the EFOE analysis. Tricyclic imine (**3**), prepared as an intermediate for the total synthesis of naturally occurring phospholipase inhibitor hispidospermidine, undergoes exclusive equatorial hydride reduction upon treatment with sodium cyanoborohydride.¹⁴ Danishefsky correctly predicted "relatively unencumbered" equatorial face (face "B" indicated

(13) Experimental procedures of these reactions followed those described in ref 12e. The stereochemical assignments of the products derived from the glycine imine or the piperazine iminium of tropone were made as follows. The stereochemistries of the products derived from the piperazine iminium were assigned by the NOESY method and the *exo/endo* ratio was determined by integration of the *N*-methyl protons ($\delta = 2.28$ for the *exo* isomer and 2.20 for the *endo* isomer) as well as the bridge head protons ($\delta = 3.19$ for the *exo* isomer and 3.08 for the *endo* isomer). The stereochemical assignment of the amine from the glycine imine, obtained as a single isomer, was made by conversion into the corresponding *endo*-piperazine derivative.

(14) Frontier, A. J.; Raghavan, S.; Danishefsky, S. J. *J. Am. Chem. Soc.* **1997**, *119*, 6686.

(15) Jones, C. D.; Kaseij, M.; Salvatore, R. N.; le Noble, W. J. *J. Org. Chem.* **1998**, *63*, 2758.

in structure **3**) to be more preferred. In agreement with his intuition, the EFOE data show that both EFOE density and PDAS value prefer equatorial attack from face "B" at **3**.



Very recently, le Noble et al. reported the stereochemistry of hydride reduction of adamantan-2-one oxonium ion and some related systems.¹⁵ Enhanced *syn* stereochemistry of NaBH₄ reduction of 2-(2-methoxy-5-fluoro-

adamantyl) cation (**4**) (*anti:syn* = 17:83) was observed. le Noble attributed this enhancement of *syn*-face selection compared with that of 5-fluoroadamantan-2-one (*anti:syn* = 37:63; NaBH₄ reduction)^{3a} to the increase of electron-demand of the carbonyl oxygen. The EFOE analysis shows significant skeletal deformation in cations **4** ($\omega = 3.6$) owing to some shrinkage of C1–C2 and C2–C3 bonds (1.527 \rightarrow 1.493 Å) compared with those of 5-fluoroadamantan-2-one ($\omega = 2.4$). As a result, face "B" is more activated toward reduction both sterically and electronically. The data of the EFOE analysis of imine **5** and iminium ion **6** were also collected for comparison.

In conclusion, the EFOE analyses of the imines and iminium ions of cyclohexanone and tropinone have revealed that the facial stereoselection of these systems is most likely to be dictated by steric effect and by the extension of LUMO. It was found that the ground-state skeletal deformation arising from the enhanced resonance effect in iminium ions is most likely to be responsible for the changes of facial stereoselection of nucleophilic additions to the systems studied.

Acknowledgment. We thank the Ministry of Education, Culture and Sports for financial support through Grants-in-Aid for Scientific Research (Project Nos. 09440215 and 09239207) and the Institute for Molecular Science for generous assignment of computational time.

JO990018W